Exosome derived from mesenchymal stem cells enhance autophagy and inhibit iNOS/TXNIP/NLRP3 inflammasome axis in injured spinal cord

Bin Lv (dr_lvbin@sina.com)
The Affliliated People's Hospital with Jiangsu University https://orcid.org/0000-0002-4368-0232
Lei Wang
The affiliated People's Hospiatal with Jiangsu University
Anquan Huang
Suzhou Municipal Hospital
Tianming Zou
Suzhou Municipal Hospital
Jishan Yuan
The Affiliated People's Hospital with Jiangsu University

Research

Keywords: Exosome;Autophagy;Spinal cord injury; Inflammasome; iNOS; TXNIP; NLRP3

Posted Date: March 11th, 2020

DOI: https://doi.org/10.21203/rs.3.rs-16805/v1

Abstract

Background: Neuroinflammation, autophagy, NLRP3 inflammasome, and microglia polarizationhave been implicated in spinal cord injury (SCI).Moreover, exosomes, a classic nanovesicles secreted by MSCs, may have a neuroprotective effect on transformation of microglia from the M1 state to the M2 phenotype. However, the effect of MSCs derived exosomes on neuroinflammation is still unclear. Here, we investigated the mechanisms of MSCs derived exosomes mediated NLRP3 inflammasome signaling cascades and its protective effects in SCI. Methods:The SCI model was performed by weight-drop impact in adult male Sprague-Dawley (SD) rats. Control andexosome rats were randomly subjecttoexosomeadminister (20 mg/kg) or placebo via intraperitoneal route 1 h after SCI.Autophagy inhibitor(3-MA) was administered intraperitoneally 20 min before experiment.Neurological function was measured by Basso-Beattie-Bresnahan (BBB) scoring and an open-field test.Neuronal death was measured by HE stainingandNisslstaining.Inducible nitric oxide synthase (iNOS) levels were determined using fluorescent probes. The autophagy and TXNIP and its downstream signaling pathways-mediated polarization of macrophages/microglia was assessed by immunohistochemistry. Results:Exosome significantly downregulated intracellular iNOS and inhibited TXNIP, pyrin domain-containing 3 (NLRP3) inflammasome pathway activation by activating autophagy. Additionally, Exosomepromoted expression of autophagy markers, such as LC3A/B and beclin1,and abrogated the expression of p62. Autophagy inhibitor, 3-MA, blockage of autophagy flux abolished the inhibition of apoptosis and iNOS/TXNIP/NLRP3 inflammasome axisafterSCI. Here, we demonstrated that exosomeadministration in spinal cord markedly reduced tissue loss, attenuate pathological morphology of the injuredregion, and promoted tissue recovery. Moreover. our resultshowed that exosome administration alleviated neuronal cells apoptosis, and inhibited nitric oxide release in microglia.The activation of inflammatoryresponse in neuronal cells facilitates interactions of iNOS-NLRP3 andTXNIP-NLRP3and inhibited NLRP3 inflammasome where neuronal cells apoptosis was induced.Further, we found that exosome could suppress macrophages/microglia polarized to M1 phenotype in vivo and in vitro.Taken together, exosome administration exerts protective effects in neuronal cells through inhibiting iNOS production, and exosome administration could inhibit iNOS/TXNIP/NLRP3 inflammasome axis via enhancing autophagy and both in vitro and in vivo. Conclusions:These resultsreveal that exosometreatment alleviatedneuroinflammation and mitigates neuronal apoptosis via autophagy-mediate inhibition of the iNOS/TXNIP/NLRP3 inflammasome axis. Our findings suggest that exosome may be a novel therapeutic target for treating SCI.

Introduction

Spinal cord injury (SCI), followed by a great many pathophysiological processes, alters its cellular environment and contributes to the resulting permanent neurological deficits[1]. Previous studies demonstrate that macroautophagy (hereafter called autophagy) is among the cellular processes altered[2,3]. Autophagy is an evolutionarily conserved lysosome-dependent degradative process response for organelles, protein aggregates, and cytoplasmic macromolecules[4]. Accumulating studies reveal that

autophagy protects against traumatically injured spinal cord via multiple mechanisms[5-7]. Meanwhile, neuroinflammatory responses, including activation of IL-1β and IL-18, play crucial roles in neural cell apoptosis[8]. Moreover, significant increases in reactive oxygen species (ROS) production have been observed in modulation of stressed neuronal cell survival, which indicate that oxidative stress and inflammation are related[9,10]. It is tempting to speculate that various neuroinflammation cytokines might interacts with ROS, mediating oxidative stress. In return, oxidative stress promotes the release of inflammatory cytokines.

Exosomes are an important paracrine factor that can be used as a direct therapeutic agent. However, there are few reports on the application of exosomes derived from bone MSCs (BMSCs-Exos) in treating SCI. Generation of pro-inflammatory mediators and propagate persistent immune signaling pathways are major components of neuroinflammational microenvironment in traumatic SCI. Oxidative stress has been considered tohavea synergetic effect on neuroinflammationin pathological progressionof the SCI[11]. Moreover, evolving evidence revealed that autophagy activation inhibited inflammasomes activation..[12-15]Thioredoxin- interacting protein (TXNIP), a pivotal regulator of the cellular redox balance, plays a crucial role in the pathogenesis of SCI. Activation of the NLRP3 inflammasome requires caspase-1, apoptosis-associated speck-like protein, and NLRP3, followed by the secretion of IL-1β and IL-18. [16]TXNIP facilitates inflammation and activates NLRP3 inflammasome forming by interacting with NLRP3. As a result, NLRP3 inflammasome remains inactive. NLRP3 inflammasomes, mainly expressed in microglia, have been reported to be regulated by various pathways, among which iNOS is a key activator[17]. Furthermore, exosome has been acknowledged as an inducer of autophagy[18].Previous study reveals that autophagy deficiency contributes to ROS accumulation [19] and exacerbation of neuroinflammation[20,21] induced by exosome. However, the role of exosome-enhanced autophagy in NLRP3 activation remains obscure. However, the role of exosome on TXNIP-mediated neuroinflammation oxidative and stress remains obscure. So we aim to investigate the role of exosome-mediated autophagy in iNOS/TXNIP/NLRP3 inflammasome axis during the process of SCI.

In the present study, we measured the effects of exosome on neuronalapoptosis,exosome-mediated autophagy,and TXNIP-NLRP3 interaction were also investigated. In addition, wealso investigated the expression of inflammatory factors in rat with SCI and the effects of exosome on microglial polarization. We demonstrated that exosome-mediated autophagy in ROS/TXNIP/NLRP3 inflammasome axis in macrophages/microglia M1-M2 polarization against SCI.

Materials And Methods

2.1 Primary neuronal culture

Primary neurons were obtained fromembryonic (d 16-18) Sprague-Dawley (SD) rats as described[22]. In brief, cerebral cortices were isolated and dissociated in trypsin (0.25%, w/v; Thermo Fisher Scientific) for 20 minutes. After incubation at 37 °C for 30 minutes to eliminate fibroblasts and glial cells, neurons were

seeded at poly-D-lysine–coated plates (Corning, Corning, NY, USA).Neurons were maintained in fresh neurobasal medium (Thermo Fisher Scientific) containing 2% B27 (Thermo Fisher Scientific), 0.5 mM glutamine (Thermo Fisher Scientific), 100 mg/ml streptomycin (Thermo Fisher Scientific), and 100 IU/ml penicillin.The collected neurons were identified by mouse anti–microtubule associated protein2(1:500; Abcam) under a fluorescence microscope.

2.2 Animals

Adult female Sprague-Dawley (SD) rats (age 8–10 week; weight, 200–250 g) were purchased from the Animal Culture Center of the Jiangsuuniversity (Jiangsu, China).All experiments were approved by Animal Committee at the Affiliated People's Hospital with Jiangsu University and conducted in accordance with the *Guide for the Care and Use of Laboratory Animals*. After anesthetized with 2% isoflurane, rats'vertebral column was exposed by incising skin and muscle.Aspinal T9 laminectomy was performed as previously described, then musclewas sewn up after administration and the fascia and skin were closed. Urination was performed three times per day manually until bladder function restored. Rats were randomly assigned into four groups: sham, SCI, SCI+exosome, and SCI+exosome+3MA. The exosome and 3MA were administered by intraperitoneal injection immediately after SCI.

2.3 Assessment of hindlimbs locomotor function

Hindlimbs locomotor function was assessed according to the Basso, Beattie, and Bresnahan(BBB) locomotor rating scale. Behavioral assessments performed by two independent observers who were blinded to treatment regimen for over five minutes at pre-injury and 1, 3, 7, 14, 21, and 28 days post-injury.

Neurologic Evaluation

BBB locomotor test was performed to evaluate the hindlimb locomotor function at pre-injury and 1, 3, 7, 14 and 21 days post SCI. The hindlimb movements during locomotion were quantified using a scale ranging from 0 to 21. Two observers, who were blinded to the group setting, observed each rat for five consecutive minutes at each time point.

Exosome isolation and identification

When BMSCs reached 80% confluency, the culture medium was replaced with exosome-depleted FBS for an additional 48 h. The medium was collected and centrifuged at 300×g for 10 min, then 2000×g for 10 min at 4 °C. Following centrifugation, a 0.22-μm sterile filter (Steritop™ Millipore, Burlington, MA) was used to filter the cell supernatant from the whole cells and cellular debris. The filtered supernatant was then applied to the upper compartment of an Amicon Ultra-15 Centrifuge Filter Unit (Millipore) and centrifuged at 4000×g until the volume was reduced to ~200 μL in the upper compartment. The ultra-filtered supernatant was then washed twice with PBS and refiltered to another 200 μL. To purify the exosomes, the liquid was loaded onto the top of a 30% sucrose/D2O cushion in a sterile Ultra-Clear™ tube (Beckman Coulter, Asphalt, CA, USA) and centrifuged at 100, 000×g for 60min at 4°C in an optima L-100 XP Ultracentrifuge (Beckman Coulter). The fraction containing the BMSC-Exos (under normoxic

conditions) was recovered using an 18-G needle, then diluted in PBS, and centrifuged at 4000×g at 4 °C in a centrifugal filter unit until the final volume reached 200 μL.

Exosomes were either stored at − 80 °C or used immediately for downstream experiments.

A Nanosight LM10 System (Nanosight Ltd., Navato, CA) was used to analyze the distribution of vesicle diameters from the Exos and HExos. The morphology of the acquired exosomes under normoxia and hypoxia was observed using a transmission electron microscope (TEM; Tecnai 12; Philips, Best, The Netherlands). Western blotting was used to determine specific exosome surface markers such as TSG101,CD9, CD63, and CD81.

BMSC-Exo protein concentration was determined using a bicinchoninic acid protein assay (BCA; Thermo Fisher Scientific, Waltham, MA). Absorbance was read at 562 nm with a microplate reader (ELx800; Bio-Tek Instruments, Inc., Winooski, VT).

Magnetic resonance imaging (MRI)

To evaluate the pathological changes in the lesion tissue, three rats in each group were randomly selected for MRI examination at day 14 post SCI. The rats were general anesthetized with halothane (3–4% induction, 1.5–2% maintenance) in nitrogen (0.6 L/min)and oxygen (0.4 L/min). To acquire the unique images on a small animal MRI system (Bruker BioSpec 7T/20 USR, Germany), rats were placed on the fixation system in the prone position to obtain a reproducible position. The sequence protocol performed with the following parameters: T2-weighted, 256×256 matrix, slice thickness 1 mm, intersection gap 1 mm, TE and TR 27/3000ms, RARE factor 16, and flip angle90 degrees. T2-weighted images were obtained in the sagittal and axial planes with ParaVision (version 6.0.1, Bruker BioSpec, Germany).

2.4 Footprint analysis

28 days post-surgery, gait and motor coordination were performed according to a previously described protocol. The front and hind paws were were soaked with ink of different colors. The rats were then placed on a strip of graph paper and encouraged to demonstrate a straight walking trace. A representative footprint pattern was then selected to analyse coordination.

2.5 Western blot analysis

Rats spinal tissues and cultured cells were collected and homogenized in ice-cold RIPA buffer RIPA buffer (89901, Thermo Scientific™, Chelmsford, MA, USA) with a phosphatase and protease inhibitor cocktail addition (Sigma-Aldrich). The sample lysates were transferred to polyvinylidene fluoride (PVDF) membranes (Millipore Corp., Billerica, MA, USA). After blocked with 10% whole milk in tris buffered saline-tween (TBST), PVDF membrane was probed with primary antibodies at 4 °C overnight. The primary antibodies were as follows: TSG101 (1:1000; Cell Signal Technology),

CD9 (1:1000; Cell Signal Technology), CD63 (1:1000; Cell Signal Technology), CD81 (1:1000; Cell Signal Technology), anti-Calpain (1:1000; Cell Signal Technology), anti-cleaved caspase-3 (1:1000; Cell Signal Technology), anti-cleaved caspase-9 (1:1000; Cell Signal Technology, USA), anti-Bcl-2 (1:1000; Abcam), anti-Bax (1:1000; Abcam), anti-GAPDH (1:1000; Abcam), anti-beclin-1 (1:1000, Cell Signaling Technology), anti-LC3(1:1000; Sigma), anti-NF200 (1:1000; Abcam), anti-mature IL-1β (1:1000; Abcam), anti-IL-1β (1:1000; Cell Signaling Technology), anti-TXNIP (1:800; Santa Cruz Biotechnology), anti-ASC (1:1000; Cell Signaling Technology), anti-NLRP3 (1:1000; Cell Signaling Technology) , anti-p62/SQSTM1 (1:1000; Abcam), anti-β-actin (1:1000; Sigma). PVDF membranes were washed with TBST buffer three times, then incubated with peroxidase-coupled secondary antibodies. Finally, PVDF membranes were visualized with ECL detection solution (Millipore, Shanghai, China).

2.5 Cell viability assessment

The cell viability was evaluated by CCK-8 assay (Dojindo Molecular Technologies, Inc.). BV-2 cells were plated in the 96-well plates (2.0 × 104 cell per well) and incubated for 24 h before experiments. The cells were washed with D-Hanks buffer solution. Two hundred microliters of CCK-8 solution was added to each well and incubated for an additional 1 h at 37 °C. The optical density (OD) of each well at 450 nm was recorded on a Microplate Reader (Thermo, Varioskan Flash). The cell viability (% of control) is expressed as the percentage of (ODtest − ODblank) / (ODcontrol −ODblank), where OD control is the optical density of the control sample and ODblank is the optical density of the wells without BV-2 cells.

The viability of HUVECs was evaluated with a CCK-8 assay (Dojindo, Kumamoto, Japan) to examine the effect of BMSCs-Exos on the proliferation of HUVEC cells. After 0, 24, 48, 72, and 96 h incubation, the wells were rinsed three times with 1 × PBS. Afterwards, CCK-8 solution (10 μL; 1:10 diluted) in fresh culture medium was added and incubated for 2 h at 37°C. Finally, the optical absorbance was measured at 450 nm using an absorbance microplate reader (ELx800, Bio-Tek, USA).

2.5 Quantification of apoptosis

A terminal deoxynucleotidyl transferase-mediated dUTP nick end labeling assay (Roche, Basel, Switzerland) was used to detect DNA fragmentation according to established protocols. After TUNEL labeling, apoptotic neuronal cells nuclei were stained with DAPI, and counted using a fluorescence microscope. The number of TUNEL positive cells, double labeled with TUNEL and DAPI, in three sections were counted and analyzed.

2.5 Nissl Staining

The 10-μm transverse frozen sections, resected from 5 mm rostral to the injury epicenter in rats of each group (n = 5), were collected for Nissl staining, 28 days post-operation. After being dried, the sections were soaked in a mixture (1:1 alcohol/chloroform) overnight. The next day, after being rehydrated with 100% alcohol, 95% alcohol, and triple-distilled water, the sections were stained with 0.1% Cresyl violet (Sigma-Aldrich, St. Louis, MO, USA) solution. The sections were subsequently differentiated in 95%

alcohol, dehydrated in anhydrous alcohol and rinsed in xylene. The number of neurons in the sections of each rat was manually counted under a light microscope. The quantity of ventral motor neurons of the section from each rat were respectively counted under a light microscope at high magnification. Then the mean number of neurons from each rat was calculated and used for subsequent analysis.

2.6 Detection of Intracellular ROS

2.7 iNOS activity assays

NOS activity was assessed as previously described protocol[23]. Briefly, primary neurons were suspended with 40μM *N*-hydroxy-L-arginine to inhibit arginase. 10 minuteslater, 20 mM L-[^{3}H]arginine was added.After two hours' interval, 0.7 M trichloroacetic acid was added. Specimen was washed with ethyl ether and passed through Dowex 50WX8 resin.Then L-[^{3}H]citrulline in the eluate was measured. The same concentration of [^{3}H]citrulline was generated if an up to 5-fold greater L-[^{3}H]arginine concentration was used, and no citrulline was detected if OG permeabilization was not performed.

2.6 Data analysis.

The data were expressed as mean ± standard deviation (SD) for n animals. Data analysis was performed by One-way ANOVA using the Prism Computerprogram (GraphPad Software Inc. San Diego, CA, USA). The relative intensity of the bands was analyzed using the Image J 1.45 software. Independent Students's t-test was used to determine differences betweengroups. Data was considered to be significant when P-value<0.05.

Result

Identification of pericytes exosomes

Exosomes derived from BMSCs were analyzed by TEM, Nano Sight particle size analysis and western blotting. Transmission electron microscopic observation showed that exosomes had the presence of spherical vesicles, with a typical cup shape. Nano-Sight particle size analysis revealed that the diameter size distribution of these nanoparticles varied from 100 to 200 nm. The specifific exosomes surface markers including CD9, CD63, CD81and TSG19 were positive in pericytes exosomes according to western blotting results, which further confifirmed the exosomes (**Figures 1a–c**).

Exosome treatment improved locomotor functional assessment and morphological evaluation of the SCI

To evaluate the neuroprotective role of exosomeon post-SCI tissue damage in vivo, we performed motor function assessments and morphological evaluation (Nissl stained sections, H&E stained sections, and MRI) to assess morphological injury in rats with a contusive injury at T10. To evaluate the hind limb locomotor function, the BBB score was recorded before SCI and 1, 3, 7, 14, 21, and 28 days post SCI. Exosome administration improved motor impairment, which showed total hindlimb paralysis (BBB score = 0) in all groups at day 1 and 3 post-SCI. However, motor function exhibited significantly sustained

improvement in the exosome group and were significantly higher than other groups throughout the test period post-SCI(Figure 2a,i).Similarly, the results of the inclined-plane test were basically consistent with the BBB scores, the maximum inclined-plane test scores in exosome group and exosome+3MA group were higher than that SCI group and Sham group from 7 days after injury the score in exosome+3MA group was smaller than that in exosome group(Figure 2a, ii). The gross morphology of the injured tissue showed that the traumatic lesion area (brown colored region) on the spinal cord was visible (Figure 2b, i). Motor coordination of forepaw-hindpaw movements decreased significantly after SCI as evaluated by walking patterns analysis, but animals treated with exosome showed a marked recovery of gait and improved motor coordination in comparison with untreated rats(Figure 2b). The lesion area in exosome group was smaller than that of the SCI group and lesion size of exosome+3MA group is in between.MRI conducted in a randomly chosen subset of each group showed remarkably reduced lesion size in the exosome group compared with the SCI group and lesion size of exosome+3MA group is in between ($p < 0.05$;Figure 2c). Histomorphology differences between groups were evaluated by HE staining and Nissl staining. Compared with other groups, exosome group showed smaller lesion area than the SCI group and lesion size of exosome+3MA group is in between. Nissl staining was utilized to examine the role of exosome on the loss of lesion tissue ($p < 0.05$; Figure 2d). MRI results confirmed revealed that exosome group presented a significantly higher percentage of preserved lesion tissue than that in other groups and lesion size of exosome+3MA group is in between ($p < 0.05$;Figure 2d).

Exosome decreases apoptosis in the spinal cord after SCI

To assess the role of exosome in modulating apoptosis after SCI,TUNEL staining andthe expression levels of apoptosis-related proteins (Bcl-2,Bax,caspase 3, andcleaved caspase 3) were evaluatedafterSCI. On the 1 day after SCI, the number of TUNEL-positive (apoptotic) cells in the SCI + exosome group was markedly lower than in the SCI group. Compared to SCI + exosome group, the apoptotic index was significantly increased after 3MA administration ($p < 0.05$; Figure 2a).Further, western blot analysis of apoptosis-related proteins showed that higher expression levels of pro-apoptotic proteins, including Bax, cleaved caspase-3, cleaved caspase-9, in the SCI group and the sham group incomparision with and SCI + exosome groups and expression levels of pro-apoptotic proteins in exosome+3MA group is in between. Similarly, exosome treatment markedly up-regulated the level of anti-apoptotic protein Bcl-2andthiseffectwasreversedinexosome+3MA group($p < 0.05$;Figure 2b).The result revealed that exosome exerted neuroprotection against SCI-induced apoptosis which could be reversed by 3MA.

Exosome inhibits neuroinflammation after SCI.

Exosome administration improves the immune microenvironment after SCI. The polarization of *macrophages/microglia* to the M1 phenotype following SCI is characterized by the release of pro-inflammatory cytokines after injury. ELISA was used to analyse the expression of the pro-inflammatory cytokines TNF-α, IL-1β, IL-2, and IFN-γ and the anti inflammatory cytokines IL-10, IL-4, and TGF-β1 in the serum of each group on the 28th day after the operation (Fig. 4a–g).

Exosome administration promotes neuronal autophagy flux and inhibits NLRP3 inflammasome after SCI.

To investigate the morphological signatures of autophagy and NLRP3 inflammasome in microglial activation, autophagy-related proteins and inflammasome were observed. Western blot analysis revealed that expression of Beclin1 and LC3B-II/ LC3B-I were significantly increased 3 d after SCI in exosome group than sham group and SCI group, besides, this phenomenon is partially reversed by 3-MA (2.14±0.02, 3.06±0.10 and 1.69±0.06, $P < 0.05$) (Figure 5c,d), while expression of p62 was significantly lower in exosome group (0.86±0.07, 0.47±0.02, and 0.71±0.02, $P < 0.05$) (Figure 5c,d). As a marker of autophagy, the ratio of LC3II/LC3I was significantly higher in the exosome treatment group than other groups (Figure 5b). To molecularly confirm the induction of autophagy, we examined the expression of autophagy by Western blot and double staining for DAPI(blue)/LC3 (green). Staining for DAPI(blue)/LC3 (green) also demonstrated that the LC3B was significantly expressed in neurons in the exosome group, and there were no significant differences between the exosome group and other groups (Figure 5a,b). These results suggest that exosome activates autophagy processes in the spinal cord following SCI.

Exosome inhibits formation of TXNIP/ NLRP3 complex post SCI.

We also examined the NLRP3-inflammasome activation in SCI. Western blot results revealed that exosome administration increases in NLRP3, cleaved-caspase-1, pro-IL-1b and IL-1b levels, but not those of ASC or pro- caspase-1. To observe the NLRP3 inflammasome in neurons, double staining for NeuN (red)/ NLRP3 (green) in lesion tissue was performed, which verified the same results. These findings revealed that the exosome administration promotes autophagy flux and inhibits NLRP3 inflammasome following SCI, while 3MA treatment corrected this phenomenon. It has been shown that thioredoxin-interacting protein was a mediator between oxidative stress and activation of the NLRP3 inflammasome. In currentstudy, weinvestigated whether exosome inhibited the NLRP3 inflammasome via regulationof TXNIP. We found that there was a significant increase of TXNIP expression in theexosome group compared with the SCI group. Inflammasome activators could induce the dissociation of TXNIP from thioredoxin in an **iNOS-sensitive manner** and the binding of TXNIP to NLRP3. We found that the 3MA significantly reversed the effects of exosome. Further, Co-IP revealed that exosome treatment enhanced TXNIP interaction with NLRP3.We verified that oxidative stress, the critical factor in NLRP3 inflammasome activation, was reduced by exosome treatment ($p < 0.05$; Figure 6).This data showed that exosome decreased the formation of the TXNIP/ NLRP3 complex and subsequently inhibited the activation of the NLRP3 inflammasome.

We found that TXNIP expression significantly increase in the SCI tissue of both the SCI, exosome, and exosome+3MA group groups compared with the control group, indicating that both TXNIP was involved in the activation of the NLRP3 inflammasome. We explored the status of the TXINP/NLRP3 inflammasome axis after SCI in each group. Following SCI, exosome inhibited the interaction of TXNIP and NLRP3 in comparision with the untreated group ($p < 0.05$; Figure 6).As shown by the increase of TXNIP/NLRP3 complex formation, traumatic SCI markedly activated the TXNIP/NLRP3 inflammasome axis in the SCI group. Exosome decreased TXNIP/NLRP3 complex formation and NLRP3 inflammasome protein levels after SCI ($p < 0.05$; Figure 6**).**

Exosome alleviates oxidative stress and the iNOS-TXNIP-NLRP3 interaction by enhancing autophagy

Consistent with this finding, the data obtained from the co-immunoprecipitation pull-down assay indicate that SCI enhanced the interaction of TXNIP and NLRP3, while exosome blocked this enhanced TXNIP NLRP3 binding (Figure 7). Accordingly, exosome increased the colocalization of NLRP3 (green) with TXNIP (red), suggesting that exosome induces the association of TXNIP with NLRP3 after SCI (Figure 7). However, pretreatment with exosome substantially suppressed the colocalization of NLRP3 with TXNIP (Figure 7). These results suggest that exosome antagonizes inflammasome activation by inhibiting TXNIP-NLRP3 interaction.

Hypothesis of the role of exosome in iNOS/TXNIP/NLRP3 inflammasome axis following SCI

Exosomes can reduce the release of proinflammatory factors in peripheral blood and the enhanced autophagy response in spinal cord tissue can weaken the activity of inflammatory corpuscles, which resulted in a severe loss of distal myelin at the proximal end of the injured area. Furthermore, exosomes improved locomotor function and restored the immune microenvironment, which conferred neuroprotection after SCI. (Figure 8)

Discussion

SCI disrupts communication between level below injury and the central system, leading to devastating disabilities.[24] It also increases iNOS production and microglial activity, which causes neuroinflammation and destructs of neurovascular vessels.[25]Numerous studies show that autophagy is a cellular digestion process that conduces to cellular homeostasis after SCI and was deemed as a potential therapeutic target.Notably, Exosome relieves neuropathic pain after SCI bypreventing dysfunction of the autophagy flux. [26]Here, our data established that administration of Exosome attenuating neuronal cell apoptosis by promoting autophagy, and its underlying mechanism of autophagy regulating iNOS/TXNIP/NLRP3 inflammasome axis. Moreover, we found that Exosomemaintain balance of M1-M2 polarization of macrophages/microglia may form a permissive environment allowing for improvement of neurological function recovery. All these factors may affect the functional recovery by limiting axonal outgrowth and preventing reformation of functional synapses.[27]

Exosome administration has been shown to attenuatemicroglial-mediated neuroinflammation and reduce neuronal damage in a SCI model[28].Furthermore, it was reported that exosomeadministration ameliorated insulin resistance by inhibiting oxidative stress in adipocytes[29]. Pandeyetal have demonstrated that exosome treatment inhibited iNOS signaling in experimental model of colitis [30]. Exosomewasalsoreportedtoinhibit mitochondrial fission and prevent ER stress-associated NLRP3 inflammasome activation[31].

Inflammasomes are intracellular signaling platforms,detecting a series of substances emerging during infections, cellular damage, or metabolic disturbances and thereby proteolytically activating the highly

proinflammatory cytokines, IL-1β, and IL-18, whereas autophagy acts as a negative regulator of inflammasomes [9]. The autophagy protein wasreportedtotargetthe ASC-containing inflammasome towards autophagosome and eventually delivered to lysosomes for destruction.[32]Moreover, it has been purported that autophagy activationcould decrease pro-IL-1β protein levels, and IL-1β is sequestered in the LC3-positive autophagosomes, indicating that pro-IL-1β direct towards autophagosome for degradation.[33]Since the exosome acts as a crucial role in autophagy andNLRP3 inflammasome, we further explored the role of exosome on autophagy in the activation of NLRP3. Activation of NLRP3 inflammasome signaling is a pivotal mediator of IL-1β function. Activation of NLRP3 is a multi-step process consisting of initial priming that up-regulates NLRP3 or pro-IL-1β expression levels, followed by activation signals leading to oligomerization and assembly of the inflammasome. After SCI, the NLRP3 inflammasome signal pathway including NLRP3, ASC, pro-caspase-1 and caspase-1 protein was activated and inflammation was induced in rats. Our resultdemonstrated that sustained exosome treatment profoundly induced NLRP3 inflammasome activation with increased expression of the key components (NLRP3, ASC, caspase-1 P20), and IL-1β activation.

TXNIP is the endogenous negative regulator of thioredoxin (TrX), which is a major cellular antioxidant and anti-apoptotic protein. Studies have revealed that elevated TXNIP expression is necessary for inducing IL-1β expression and acting as a binding partner for NLRP3 in microglia.[34] Under oxidative stress conditions, TXNIP dissociates from TrX and allows the binding of TXNIP to NLRP3, which contributes to the formation and activation of the inflammasome. Furthermore, Zhou and colleagues identified TXNIP as a critical link between oxidative stress and inflammasome activation using cultured macrophages or TXNIP knockout mice. The assembly of the NLRP3 inflammasome controls the process and production of the pro-inflammatory, cytokine IL-1β. The SCI tissues samples showed remarked increases in the levels of TXNIP protein expression

As is common knowledge, microglia is the main source of pro-inflammatory cytokines in the lesion tissue. The activation of microglia may have detrimental effects on neurons by expressing and synthesizing pro-inflammatory cytokines such as IL-1β,which induces neuroinflammation.We examined the role played by exosome in regulating iNOS/TXNIP/NLRP3 inflammasome axis. Further, we examined role ofautophagyinhibitionin altering pro-inflammatory IL-1β, IL-6 and TNF-α, and aiNOS production. In this study, our data proved that Exosome upregulates LC3 and Beclin 1 and attenuates iNOS and iNOS-regulated Txnip in the SCI, linking inflammasome and oxidative stress.We believe that the inhibition of NLRP3 inflammasomes activation by Exosome should be attribute toits inhibitory effects on iNOS. Enhancement of autophagy reduces TXNIP protein expression and suppresses TXNIP-NLRP3 interaction,the decreased oxidative stress after Exosomeadministration could inhibiting macrophages/microglia polarization to M1 phenotype after SCI.

Traumatically injured spinal cord can activatemicroglia andstimulate the activation of M1 macrophages and activated, M2a, M2b, and M2c macrophages occurs in different phases of repair[35]. These phenotypes exert respective roles in certain pathological processes after SCI. The inflammatory phase consists ofM1 macrophages/microglia polarization, which impedes the healing process of SCI. Exosome,

a compound acting as anti-oxidative and anti-inflammatory, has been demonstrated to play a neuroprotective role in inhibiting inflammatory response. Here, we revealed thatExosomedecreased the number of M1-type macrophages/microglia phenotype, while increased the number of M2-type macrophages/microglia.

Previous study has shown that limiting inflammation contribute to inhibition of M1 macrophage polarization and thus to suppress M2 macrophage polarization in pathological progress of SCI. Yao et al. reported that programmed death 1 deficiency induces the polarization of macrophages/microglia to the M1phenotype after traumatical SCI.Our study provided evidence that Exosomeswitch cell polarization from M1 to the M2 phenotype and provides neuroprotection through autophagy-mediate inhibitionofiNOS/TXNIP/NLRP3 inflammasome axis induced by M1 macrophages/microglia.

In current study, we investigated the effect of Exosome on SCI and the relationship between autophagy and iNOS/TXNIP/NLRP3 inflammasome axis with their associated mechanisms, after Exosome administration in SCI. Moreover, Exosome administration activated the autophagy process by improveingexpression level of the autophagy-related proteins and attenuated the iNOS/TXNIP/NLRP3 inflammasome axis activation. Increasing autophagy and inhibiting inflammasome by Exosome administration may exert the neuroprotective role of Exosome in SCI. Meanwhile, inhibiting autophagy by 3-MA administration reversed the neuroprotective effect. Further, inflammasome related protein was proved to be downstream of autophagy.

Conclusions

In summary, we suggested that Exosome could alleviate traumatical SCI by promoting autophagy mediated inactivation of iNOS/TXNIP/NLRP3 inflammasome axis. We suppose the Exosome administration can be a novel therapeutic avenue in treating SCI.

Abbreviations

iNOS: Inducible nitric oxide synthase;SD: Sprague-Dawley;

TrX: thioredoxin; Co-IP: coimmunoprecipitation; SD: standard deviation;

MRI: Magnetic resonance imaging; TXNIP: Thioredoxin- interacting protein

BBB: Blood-brain barrier; SCI: Spinal cord injury; Exos: Exosomes

MSCs: Mesenchymal stem cells; SCI: Spinal cord injury;

Declarations

Acknowledgements

Not applicable.

Authors' contributions

BL and JSY designed and supervised this study. BL, LW, and AQH conducted the majority of the experiments and completed the manuscript. AQH and THZ analyzed the data. BL and LW participated the experiments and the manuscript writing. BL, LW, and AQH participated in editing the manuscript. BL and LW produced the spinal cord injury model. All authors approved the final version of the manuscript.

Funding

This work was sponsored by the National Natural Science Foundation of China (GrantNo.81772352),Clinical Medicine Science and Technology Development Foundation of Jiangsu University (Grant No: JLY20180047),Zhenjiang Science & Technology Program (Grant No: SH2019085).

Availability of data and materials

Most of the datasets supporting the conclusions of this article are included within this article and the additional files. The datasets used or analyzed during the current study are available on reasonable request.

Ethics approval and consent to participate

All animal procedures were performed under the guidelines of the institutional review board and the ethics committee of Jiangsu University.

Consent for publication

Not applicable.

Competing interests

The authors declare that they have no competing interests.

References

1 Yacoub, A. *et al.* Neuroprotective effects of perflurocarbon (oxycyte) after contusive spinal cord injury. *J Neurotrauma* **31**, 256-267, doi:10.1089/neu.2013.3037 (2014).

2 Kanno, H., Ozawa, H., Sekiguchi, A. & Itoi, E. The role of autophagy in spinal cord injury. *Autophagy* **5**, 390-392 (2009).

3 Motori, E. *et al.* Inflammation-induced alteration of astrocyte mitochondrial dynamics requires autophagy for mitochondrial network maintenance. *Cell metabolism* **18**, 844-859, doi:10.1016/j.cmet.2013.11.005 (2013).

4 Levine, B. & Kroemer, G. Autophagy in the pathogenesis of disease. *Cell* **132**, 27-42, doi:10.1016/j.cell.2007.12.018 (2008).

5 He, M. *et al.* Autophagy induction stabilizes microtubules and promotes axon regeneration after spinal cord injury. *Proceedings of the National Academy of Sciences of the United States of America* **113**, 11324-11329, doi:10.1073/pnas.1611282113 (2016).

6 Houtman, J. *et al.* Beclin1-driven autophagy modulates the inflammatory response of microglia via NLRP3. *EMBO J* **38**, doi:10.15252/embj.201899430 (2019).

7 Bai, L. *et al.* The Role of Netrin-1 in Improving Functional Recovery through Autophagy Stimulation Following Spinal Cord Injury in Rats. *Front Cell Neurosci* **11**, 350, doi:10.3389/fncel.2017.00350 (2017).

8 Thomas, C. A. *et al.* Modeling of TREX1-Dependent Autoimmune Disease using Human Stem Cells Highlights L1 Accumulation as a Source of Neuroinflammation. *Cell stem cell* **21**, 319-331.e318, doi:10.1016/j.stem.2017.07.009 (2017).

9 Gupta, M. & Kaur, G. Aqueous extract from the Withania somnifera leaves as a potential anti-neuroinflammatory agent: a mechanistic study. *J Neuroinflammation* **13**, 193, doi:10.1186/s12974-016-0650-3 (2016).

10 Alhazzani, A. *et al.* Mesenchymal Stem Cells (MSCs) Coculture Protects [Ca(2+)]i Orchestrated Oxidant Mediated Damage in Differentiated Neurons In Vitro. *Cells* **7**, doi:10.3390/cells7120250 (2018).

11 Pitarokoili, K. *et al.* Intrathecal triamcinolone acetonide exerts anti-inflammatory effects on Lewis rat experimental autoimmune neuritis and direct anti-oxidative effects on Schwann cells. *J Neuroinflammation* **16**, 58, doi:10.1186/s12974-019-1445-0 (2019).

12 Schwartz, D. M. *et al.* JAK inhibition as a therapeutic strategy for immune and inflammatory diseases. *Nature reviews. Drug discovery* **16**, 843-862, doi:10.1038/nrd.2017.201 (2017).

13 Beck, K. D. *et al.* Quantitative analysis of cellular inflammation after traumatic spinal cord injury: evidence for a multiphasic inflammatory response in the acute to chronic environment. *Brain* **133**, 433-447, doi:10.1093/brain/awp322 (2010).

14 Witcher, K. G. *et al.* Traumatic brain injury-induced neuronal damage in the somatosensory cortex causes formation of rod-shaped microglia that promote astrogliosis and persistent neuroinflammation. *Glia* **66**, 2719-2736, doi:10.1002/glia.23523 (2018).

15 He, W. *et al.* Hypothermic oxygenated perfusion (HOPE) attenuates ischemia/reperfusion injury in the liver through inhibition of the TXNIP/NLRP3 inflammasome pathway in a rat model of donation after cardiac death. *FASEB J*, fj201800028RR, doi:10.1096/fj.201800028RR (2018).

16 He, Y., Hara, H. & Nunez, G. Mechanism and Regulation of NLRP3 Inflammasome Activation. *Trends in biochemical sciences* **41**, 1012-1021, doi:10.1016/j.tibs.2016.09.002 (2016).

17 Ichinohe, T., Yamazaki, T., Koshiba, T. & Yanagi, Y. Mitochondrial protein mitofusin 2 is required for NLRP3 inflammasome activation after RNA virus infection. *Proceedings of the National Academy of Sciences of the United States of America* **110**, 17963-17968, doi:10.1073/pnas.1312571110 (2013).

18 Saladini, S. *et al.* Metformin Impairs Glutamine Metabolism and Autophagy in Tumour Cells. *Cells* **8**, doi:10.3390/cells8010049 (2019).

19 A, L. *et al.* Defective CFTR induces aggresome formation and lung inflammation in cystic fibrosis through ROS-mediated autophagy inhibition. *Nature cell biology* **12**, 863-875 (2010).

20 B, d. L.-D. *et al.* Melatonin reduces endoplasmic reticulum stress and autophagy in liver of leptin-deficient mice. *Journal of pineal research* **61**, 108-123 (2016).

21 Lotfi, P. *et al.* Trehalose reduces retinal degeneration, neuroinflammation and storage burden caused by a lysosomal hydrolase deficiency. *Autophagy* **14**, 1419-1434, doi:10.1080/15548627.2018.1474313 (2018).

22 Takei, N. *et al.* Brain-derived neurotrophic factor induces rapid and transient release of glutamate through the non-exocytotic pathway from cortical neurons. *J Biol Chem* **273**, 27620-27624 (1998).

23 Thom, S. R., Bhopale, V. M. & Yang, M. Neutrophils generate microparticles during exposure to inert gases due to cytoskeletal oxidative stress. *J Biol Chem* **289**, 18831-18845, doi:10.1074/jbc.M113.543702 (2014).

24 Jayaprakash, N. *et al.* Optogenetic Interrogation of Functional Synapse Formation by Corticospinal Tract Axons in the Injured Spinal Cord. *The Journal of neuroscience : the official journal of the Society for Neuroscience* **36**, 5877-5890, doi:10.1523/jneurosci.4203-15.2016 (2016).

25 von Leden, R. E., Khayrullina, G., Moritz, K. E. & Byrnes, K. R. Age exacerbates microglial activation, oxidative stress, inflammatory and NOX2 gene expression, and delays functional recovery in a middle-aged rodent model of spinal cord injury. *J Neuroinflammation* **14**, 161, doi:10.1186/s12974-017-0933-3 (2017).

26 Weng, W. *et al.* Metformin relieves neuropathic pain after spinal nerve ligation via autophagy flux stimulation. *J Cell Mol Med* **23**, 1313-1324, doi:10.1111/jcmm.14033 (2019).

27 Chen, B. *et al.* Reactivation of Dormant Relay Pathways in Injured Spinal Cord by KCC2 Manipulations. *Cell* **174**, 521-535 e513, doi:10.1016/j.cell.2018.06.005 (2018).

28 Pan, Y. *et al.* Metformin reduces morphine tolerance by inhibiting microglial-mediated neuroinflammation. *J Neuroinflammation* **13**, 294, doi:10.1186/s12974-016-0754-9 (2016).

29 Qiu, J. *et al.* NYGGF4 (PID1) effects on insulin resistance are reversed by metformin in 3T3-L1 adipocytes. *Journal of bioenergetics and biomembranes* **44**, 665-671, doi:10.1007/s10863-012-9472-x (2012).

30 Pandey, A., Verma, S. & Kumar, V. L. Metformin maintains mucosal integrity in experimental model of colitis by inhibiting oxidative stress and pro-inflammatory signaling. *Biomed Pharmacother* **94**, 1121-1128, doi:10.1016/j.biopha.2017.08.020 (2017).

31 Li, A. *et al.* Metformin and resveratrol inhibit Drp1-mediated mitochondrial fission and prevent ER stress-associated NLRP3 inflammasome activation in the adipose tissue of diabetic mice. *Mol Cell Endocrinol* **434**, 36-47, doi:10.1016/j.mce.2016.06.008 (2016).

32 Shi, C. S. *et al.* Activation of autophagy by inflammatory signals limits IL-1beta production by targeting ubiquitinated inflammasomes for destruction. *Nature immunology* **13**, 255-263, doi:10.1038/ni.2215 (2012).

33 Harris, J. *et al.* Autophagy controls IL-1beta secretion by targeting pro-IL-1beta for degradation. *J Biol Chem* **286**, 9587-9597, doi:10.1074/jbc.M110.202911 (2011).

34 Chen, D. *et al.* IRE1alpha inhibition decreased TXNIP/NLRP3 inflammasome activation through miR-17-5p after neonatal hypoxic-ischemic brain injury in rats. *J Neuroinflammation* **15**, 32, doi:10.1186/s12974-018-1077-9 (2018).

35 Zhang, Y. *et al.* Melatonin improves functional recovery in female rats after acute spinal cord injury by modulating polarization of spinal microglial/macrophages. *J Neurosci Res* **97**, 733-743, doi:10.1002/jnr.24409 (2019).

Figures

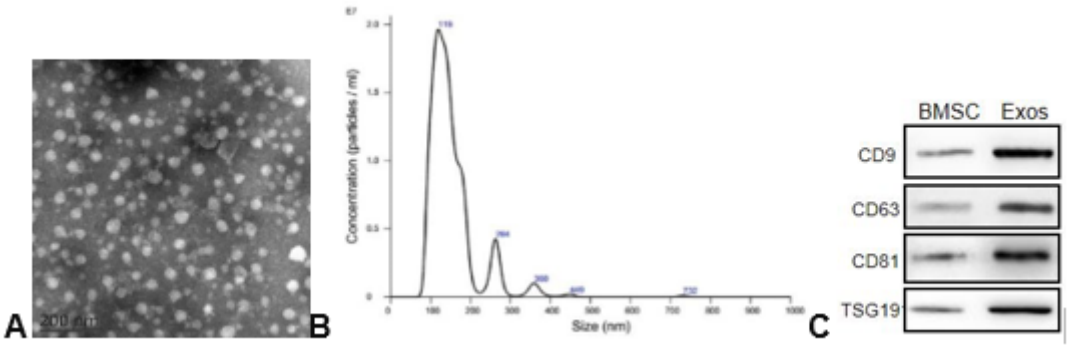

Figure 1

Characterization of BMSC-derived exosomes (Exos). (a) Morphology of Exos revealed by transmission electron microscopy (TEM). (b) Particle size distribution measured by NTA analysis. (c) Western blot analysis of specific exosomal surface markers including TSG101, CD9, CD63 and CD81.

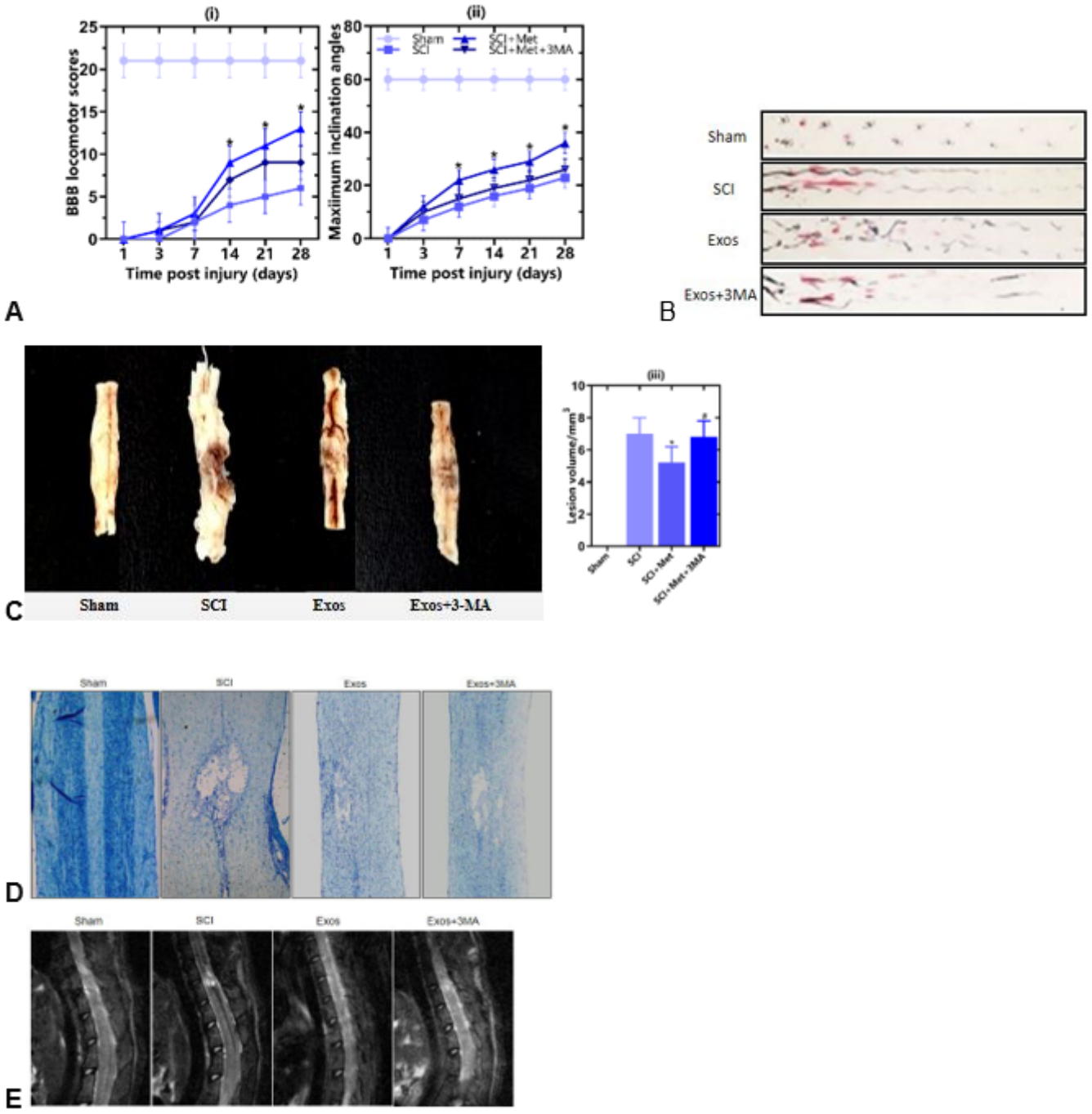

Figure 2

Exosome treatment improved locomotor functional assessment and morphological evaluation of the injured spinal cord post-SCI. (a,i) The rats were functionally graded up to 28 days post injury using the BBB grading scale;(a,ii) The rats were functionally graded up to 28 dayspost injury using the inclined-plane-test angles of rats. (b, i) Representative footprints of an animal walking 28 days after SCI. Blue:

front paw print; red: hindpaw print.(c)Representative images of spinal cordinrats at 28 days post injury; (b, iii) Gross morphology and the lesion volumes (mm3) of spinal cord. (c) Gross morphology of spinal sections.(d) H&E stained and Nissl stained sagittal sections.(e)Representative sagittal MRI images.*p < 0.05 compared to the SCI group, #p < 0.05 compared with the SCI +Exosome group, SCI: spinal cord injury; BBB: Basso-Beattie-Bresnahan. All data are presented as mean±SEM, N=3. The level of significance was set at *P <0.05.

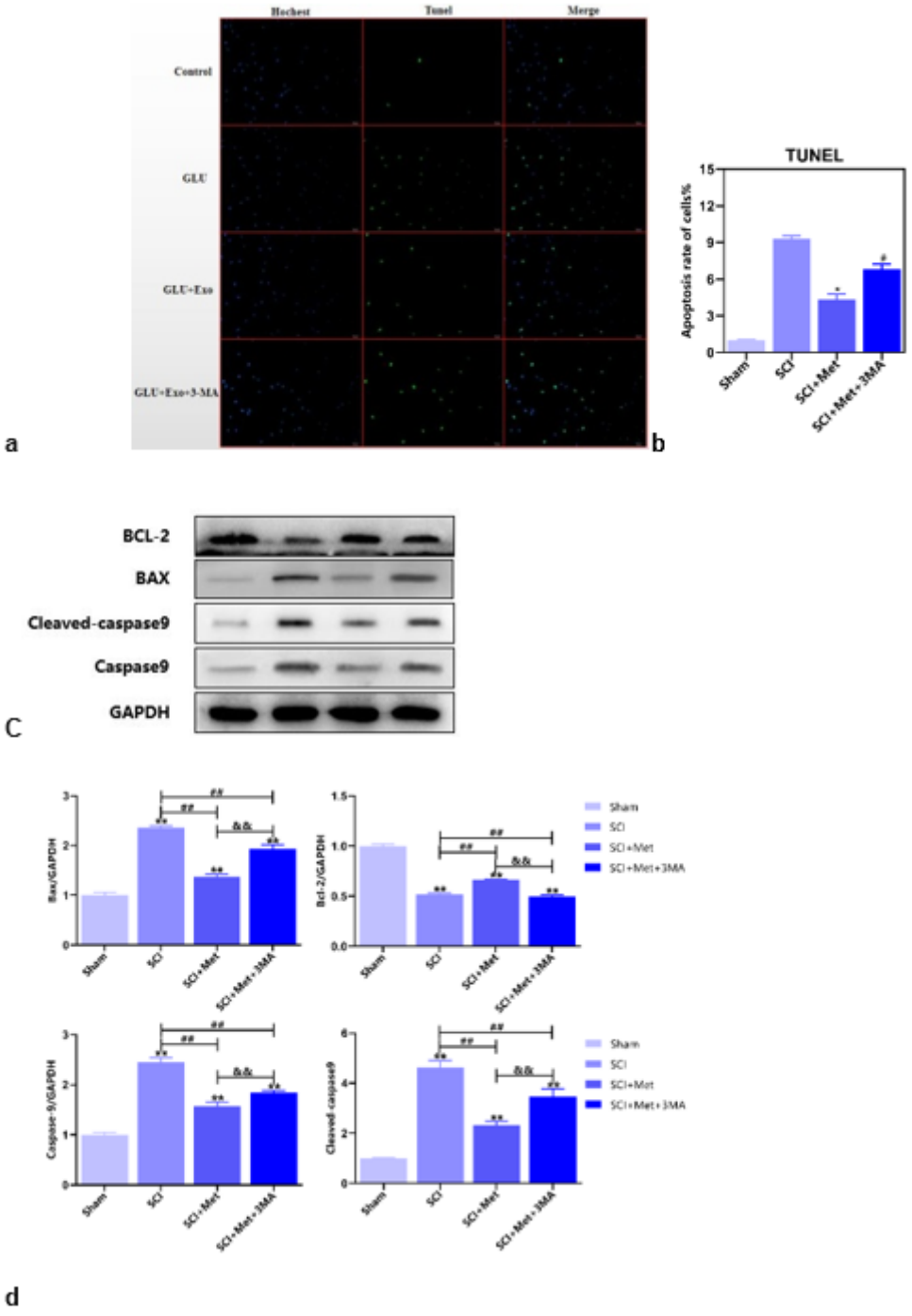

Figure 3

Neuroprotective manner of exosome administration on neuronal apoptosis post-SCI in vitro. (a) Representative immunofluorescence images of TUNEL (green) and nuclei (blue) staining in primary rat spinal cord neurons on first day post SCI. (b) Quantification of the number of TUNEL (green)-positive cells in (a). (c) The expression of apoptosis-associated proteins on first day post SCI, as demonstrated by Western blotting. (d) Semiquantitative analysis of relative expression level of apoptosis-related proteins, normalized to GAPDH. All data are presented as mean ± SEM, N=3,The level of significance was set at *P < 0.05.

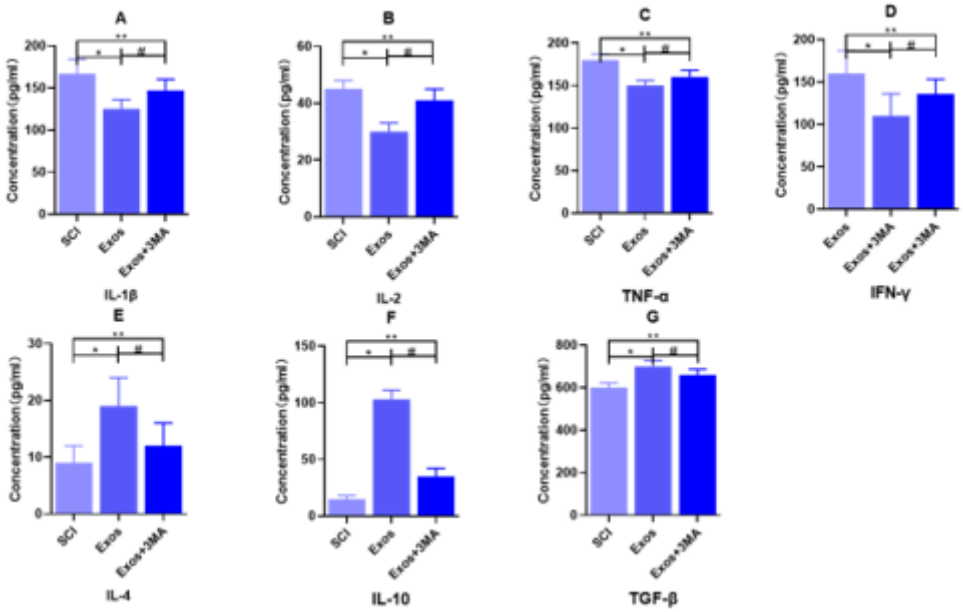

Figure 4

Exosome administration promotes changes in peripheral serum inflammation after SCI. (a–d) Changes in the levels of thepro-inflammatory cytokines IL-1β, IL-2, TNF-α, and IFN-γ, n = 3. e–g Changes in the levels of the anti-inflammatory cytokines IL-4, IL-10, and TGF-β1, n = 3. All data are expressed as mean ± SEM. N=3, The level of significance was set at *P < 0.05.

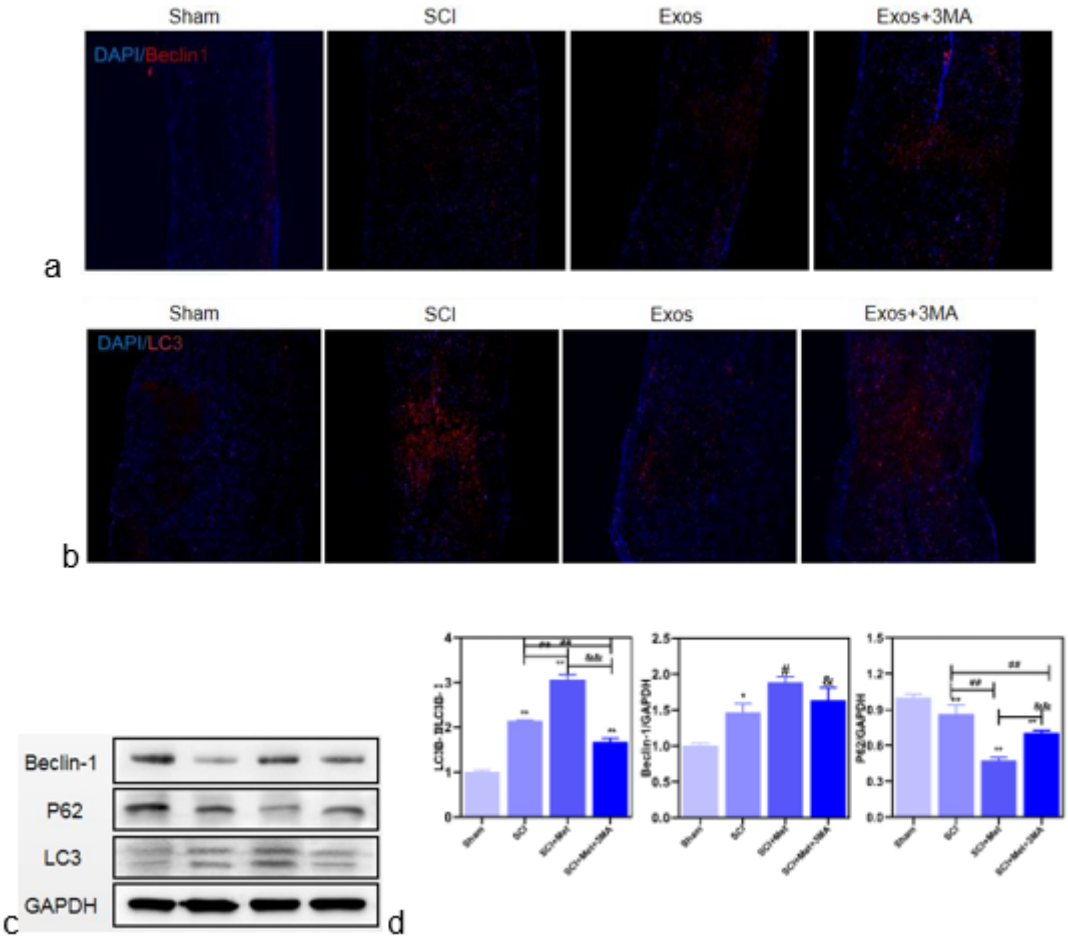

Figure 5

Immunofluorescence and western blot analysis of beclin-1 and LC3B expression in spinal cord following injury. a, b Numbers of beclin-1/DAPI positive neurons in spinal sections as determined by fluorescence microscopy. Beclin-1-positive (autophagic) neurons were significantly more numerous in the exosome group than the SCI group. c, d Number of LC3B/DAPI double-positive neurons. LC3Bpositive neurons were also significantly more numerous in the SCI + exosome group. e Western blot analysis of autophagy-related proteins at 6 and 24 h after SCI. f)Semi-quantitative analysis showing significantly greater expression levels of autophagy-related proteins in the exosome group than the SCI group. Expression was normalized to GAPDH. *p < 0.05 compared with the Sham group, #p < 0.05 compared with the SCI group.

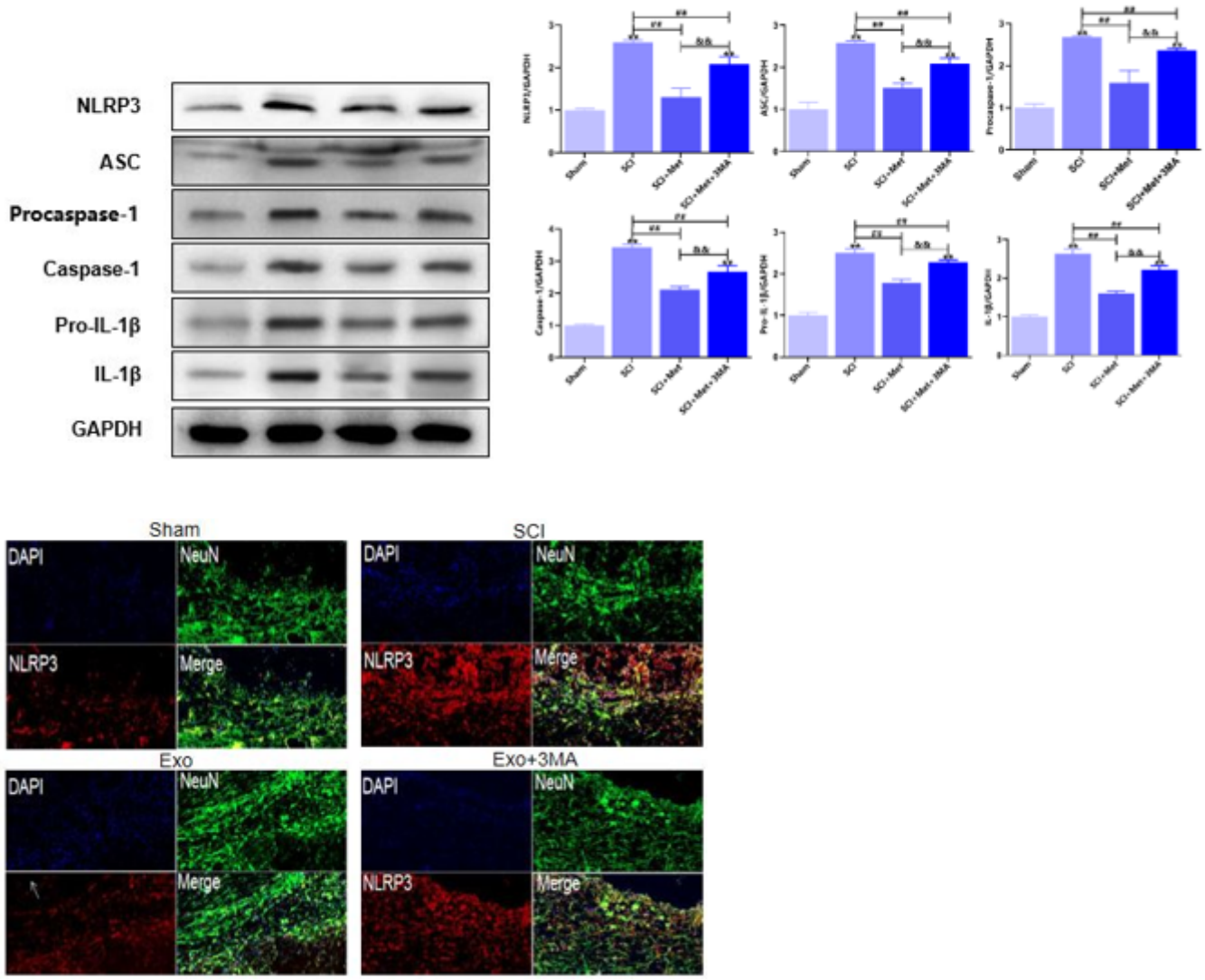

Figure 6

Exosome administration promotes neuronal autophagy and inhibits NLRP3 inflammasome activity in the spinal cord after injury. (a) Protein expressions of Beclin-1, p62, and LC3II/I of rats in sham, SCI and SCI + Exo groups were analyzed using Western blotting, respectively. (b) Quantitative estimation of autophagy-related proteins normalized to GAPDH. (c) Distribution of LC3 (green) immunoreactivity in the spinal cord following injury. (d) Tissues were housed and protein expressions of NLRP3, ASC, procaspase1, caspase-1, pro-IL-1β, and IL-1β proteins were analyzed with real-time PCR. *P < 0.05, compared to the sham group; #P < 0.05, compared to SCI group;&P < 0.05, compared to SCI+Exogroup; All data are presented as mean ± SEM, N=3,The level of significance was set at *P < 0.05.

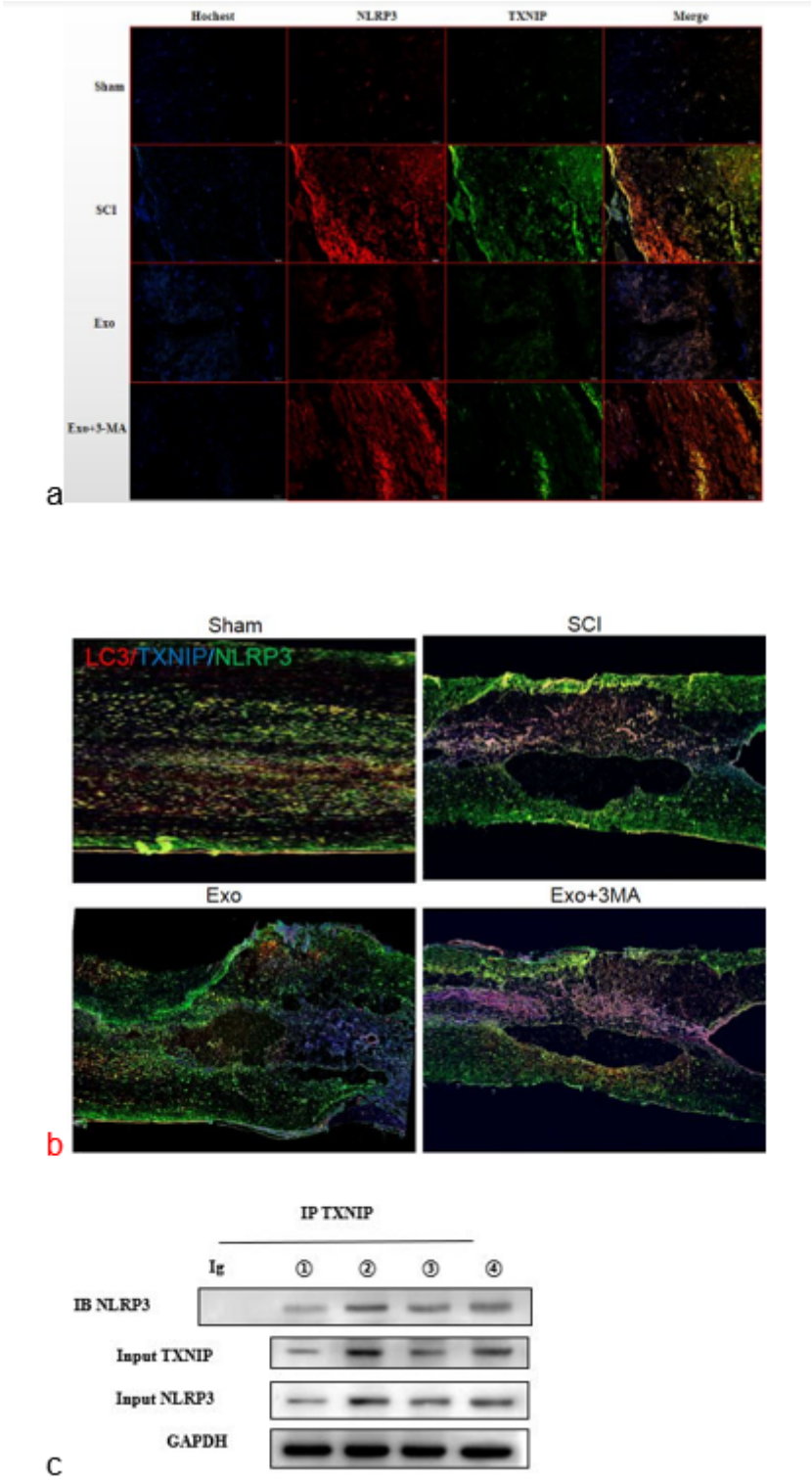

Figure 7

Exosome administrationinhibits the interaction of TXNIP and NLRP3 and microglial activationpost SCI. (a)The colocalization of TXNIP with NLRP3 in spinalcord wasvisualized by confocal microscopy. (b) NLRP3 (blue) and iNOS (red) of lesion tissues were estimated through immunofluorescence staining. (c)the interaction of TXNIP/NLRP3 were determined by coimmunoprecipitation (Co-IP) in each group post SCI. All data are expressed as mean±SEM, n =3. The level of significance was set at *P < 0.05.

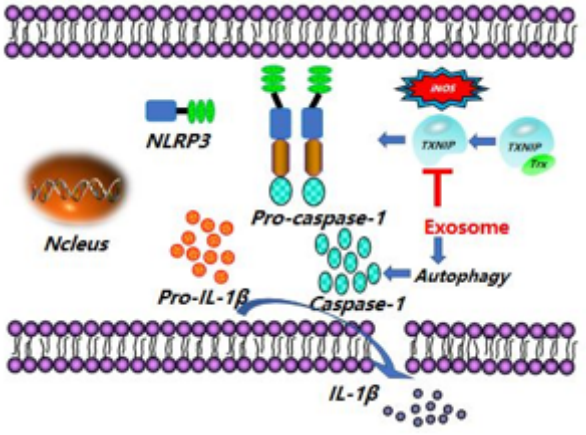

Figure 8

Schematic diagram showing the proposed protective effects of exosome in inhibiting iNOS/TXNIP/NLRP3 inflammasome axis mediated by autophagy.